ARTICLES

Ionization of Amino-, Thio- and Hydroxy-naphtalenes via Free (Unhindered) Electron Transfer

Aliaksandr Baidak,[†] Sergej Naumov,[‡] Ralf Hermann,[†] and Ortwin Brede*,[†]

Interdisciplinary Group Time-resolved Spectroscopy, University of Leipzig, Permoserstrasse 15, 04303 Leipzig, Germany, and Leibniz Institute of Surface Modification, Permoserstrasse 15, 04303 Leipzig, Germany

Received: April 30, 2008; Revised Manuscript Received: September 1, 2008

The electron transfer from various monosubstituted naphthyl derivatives (naphtols, NpOH; naphtylamines, $NpNH_2$; and thionaphtols, NpSH) to parent n-BuCl radical cations was studied by means of pulse radiolysis. The experiments reveal the synchronous and direct formation of two types of transients: the metastable solute radical cation ($NpXH^{\bullet+}$, X = heteroatom) and the corresponding heteroatom-containing radical ($NpX^{\bullet}$) in comparable amounts. This is explained in terms of the free (unhindered) electron transfer in nonpolar solvents, which is a bimolecular process reflecting femtosecond time scale events of intramolecular dynamic motions accompanied by significant changes of the electron distribution within the donor molecule.

Introduction

In recent years much work has been done on the electron transfer phenomenon called free electron transfer (FET).[1] FET stands for an electron transfer process where the molecule oscillations of the donor are reflected in a bimolecular reaction. This is reasoned by an unhindered electron jump proceeding in the first encounter of the reactants. So "free" means unhindered and concerns the transfer, not the electron.

In general, FET represents the bimolecular electron transfer from donor molecules to parent radical cations derived from nonpolar solvents such as n-alkanes,[2] cycloalkanes,[3] and alkyl chlorides.[4] These radical cations are able to oxidize a large variety of organic molecules due to the high ionization potentials of the solvents used (IP $\approx$ 9.5−10.9 eV[5]), for example, reactions 1 and 2. Electron pulse radiolysis is a key technique for the observation of such processes.

$$RX - \text{e-beam} \rightarrow RX^{\bullet+} + e_{solv}, \text{ radicals, etc. } X = H, Cl \qquad (1)$$

$$RX^{\bullet+} + D \rightarrow RX + D^{\bullet+} \quad D = \text{donor molecule} \qquad (2)$$

Radical ions are weakly solvated in nonpolar media. Hence, in a rough approximation, their interaction with the solvent molecules might be neglected. This is supported by the observation of the high mobility of the solvent radical cations ("hopping") in nonpolar media.[6,7]

In spite of logical prediction that the donor radical cation is the only product of FET from the donor to the solvent radical cation, a surprising two-product situation has been observed in experiments involving phenols, thiophenols, selenols, aromatic amines, and aromatic silanes, as summarized in a feature article.[1] In other words, a synchronous and immediate formation of the radical cations and of the corresponding radicals has been found.

This unusual observation was interpreted in terms of molecular dynamics, where intramolecular dynamic motions of the donor molecules, such as bending (rotation), are taken into consideration. With quantum chemical calculations it can be shown for the aromatic molecules substituted with heteroatom-containing groups that the rotational motion of the substituent toward the aromatic ring is connected with the shifts of the electron density, which justifies the definition of the donor molecules as a dynamic mixture of rotational conformers.

Now it should be taken into account that the ion−molecule reaction of FET (eq 2) consists of several steps as subsequently formulated (eq 3).

$$RCl^{\bullet+} + D \underset{\text{diffusion}}{\rightleftharpoons} RCl^{\bullet+}\cdots D \underset{\text{e-jump}}{\rightleftharpoons} RCl\cdots D^{\bullet+} \underset{\text{diffusion}}{\rightleftharpoons} RCl + D^{\bullet+} \qquad (3)$$

It is assumed that because of the weak solvation shell and the high free energy of reaction 2 that the actual electron jump proceeds directly in the first encounter of the reactants. If so, then the electron jump happens in the subfemtosecond time range, that is, it is much faster than molecular motions.[8] Obviously, under such circumstances the very primary products of the ionization preserve the same geometry as their neutral precursors. Hence, the spin distribution in the formed radical cations reflects the electron distribution in the ground-state of the corresponding rotational conformers. Scheme 1 describes ionization of phenol via FET.

For the variety of dynamic conformers, a necessary simplification allows reduction of the conformer situation to the two extreme cases such as a planar (a) and a twisted (b) one. The planar structure with efficient electron delocalization over the whole molecule gives rise to the metastable radical cation. Commonly, the twisted conformer with an electron density preferably localized on the heteroatom relates to the unstable, dissociative radical cation, which deprotonates immediately after its formation.

In all the cases, when heteroatom-substituted aromatic molecules exhibit pronounced bending motions, the bimolecular

* Corresponding author e-mail: brede@mpgag.uni-leipzig.de.
[†] University of Leipzig.
[‡] Leibniz Institute of Surface Modification.

10.1021/jp806711m CCC: $40.75
Published on Web 10/15/2008

SCHEME 1: Formation of Two Types of Radical Cations (Planar, Metastable (a) and Twisted, Dissociative (b)) upon Ionization of Phenol in n-Butyl Chloride Solution

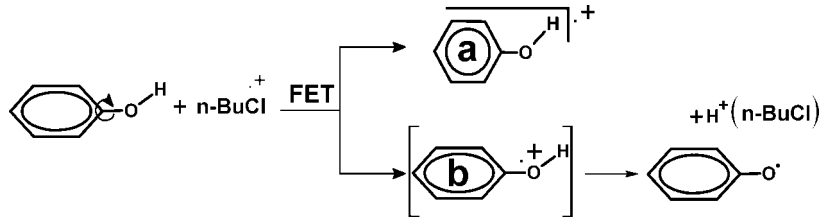

electron transfer process leads to the immediate formation of two different products: radical cation and the corresponding radical. Immediate dissociation of the unstable radical cation may manifest itself not only as a deprotonation, but also a release of other good leaving groups, such as $(CH_3)_3Si^+$ or $(CH_3)_3C^+$.[9,10]

To investigate the FET behavior of the electron donors with larger, compared to benzene, aromatic moieties, pulse radiolysis studies with different naphthyl derivatives have been done. For this purpose, naphtols (α- and β-), naphtylamines, and thionaphtols were used. An extended aromatic moiety should increase the stability of radical cations in comparison to benzene analogues and, therefore, improve the kinetic analysis of the FET phenomenon. Although some test experiments[11,12] were already described, we performed a systematic study of naphtyl-containing donors in order to get a deeper insight into the FET matter.

Experimental Section

Pulse Radiolysis. Pulse radiolysis[13] experiments were carried out using a pulse-transformer-type accelerator ELIT (Institute of Nuclear Physics, Novosibirsk, Russia). The liquid samples, purged with nitrogen or oxygen, were irradiated with high-energy electron pulses (1 MeV, 15 ns pulse duration). The absorbed dose per pulse was measured with an electron dosimeter (absorption of a solvated electron in water at 580 nm). The dose delivered per pulse was usually around 100 Gy, which corresponds to transient concentration around 10^{-5} mol dm^{-3} of the primary n-$BuCl^{\bullet+}$. The detection of the transient species was performed using an optical absorption setup. It consists of a pulsed xenon lamp (XBO 450, Osram), a spectra Pro-500 monochromator (Acton Research Corporation), a R9220 photomultiplier (Hamamatsu Photonics), and a 1 GHz digitizing oscilloscope (TDS 640, Tektronix). All experiments were carried out in n-butyl chloride solutions. Only freshly prepared solutions were used. The solutions continuously flowed though the sample cell with an optical path length of 1 cm. In some cases a cutoff filter (at 320 nm) was used in order to avoid possible side reactions caused by the UV light irradiation.

Chemicals. 1- and 2-Naphtol (99%), 1-and 2-napthylamine (95%), and 1 and 2-thionaphtol (99%) were purchased from Aldrich and were used as received. n-Butyl chloride of the highest commercially available purity (Merck) was used without additional purification.

Results

Pulse radiolysis of n-BuCl results in the formation of solvent radical cation[4] as well as less reactive radicals (reaction 4).

$$\text{BuCl}-\text{e-beam} \rightarrow \text{BuCl}^{\bullet+} + \text{Bu}^{\bullet} + \text{Cl}^{-} \qquad (4)$$

The n-$BuCl^{\bullet+}$ radical cation shows a broad optical absorption band with a maximum around 500 nm.[4] The lifetime of $BuCl^{\bullet+}$ is approximately 100 ns. In the presence of a quencher (compound with lower ionization potential in comparison to the parent radical cation) in millimolar concentration, the solvent radical cations $BuCl^{\bullet+}$ undergo a diffusion-controlled electron transfer reaction (analogous to reaction 2). As a result, the lifetime of the parent radical cation is reduced to a few nanoseconds. The rate constant of the FET was found to be in the range $(1-2) \times 10^{10}$ dm^3 mol^{-1} s^{-1}.

Pulse Radiolysis of 2- and 1-Naphtylamine. The rate constant of the free electron transfer from 2-naphtylamine (2-$NpNH_2$) to the solvent radical cations (cf. reaction 5) was determined from the decay of the solvent radical ions in the presence of different 2-$NpNH_2$ concentrations ($0.5-1.5 \times 10^{-3}$ mol dm^{-3}) so that the FET reaction 5 followed pseudofirst-order reaction kinetics. The rate constant obtained from the Stern−Volmer-type plot amounts to $k_5 = 2 \times 10^{10}$ dm^3 mol^{-1} s^{-1}.

$$\text{BuCl}^{\bullet+} + \text{2-NpNH}_2 \rightarrow \text{BuCl} + \text{2-NpNH}_2^{\bullet+} \qquad (5)$$

Figure 1 shows the transient optical absorption spectra taken in the pulse radiolysis of a N_2-saturated solution of 2-$NpNH_2$ (5×10^{-3} mol dm^{-3}) in n-BuCl.

At early times (100 ns after the pulse), the transient spectrum exhibits at least two absorption bands, at 370 nm and in the 500−570 nm range. After this time the solvent radical cations were already consumed by the free electron transfer reaction (5). It means that the spectra registered with time delay of more then 100 ns after the electron pulse are caused exclusively by the transient species derived from 2-$NpNH_2$. The broad absorption band at 500−570 nm is a result of superposition of the absorption bands of two different intermediates. These species are distinguishable due to their different kinetic behavior (cf. difference spectrum in Figure 1 and time profiles given as inset). A short living transient exhibits an absorption maximum at λ_{max} = 550 nm, and a longer living one has its maximum at 510

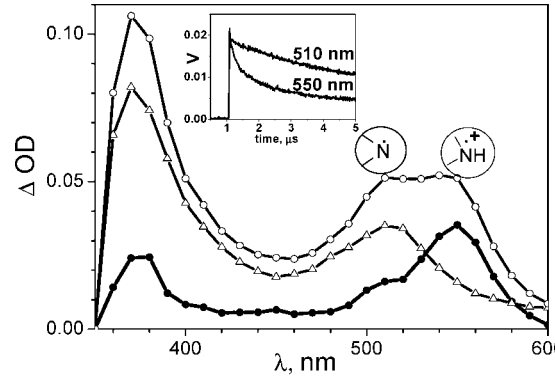

Figure 1. Transient optical absorption spectra obtained in the pulse radiolysis of N_2-saturated solution of 2-$NpNH_2$ (5×10^{-3} mol dm^{-3}) in BuCl. Spectra correspond to times (○) 100 ns and (Δ) 2.1 μs. The spectrum of the radical cation (●) is presented as a difference between (○) and (Δ). Experimental time profiles taken in the maxima of the absorption bands are given as inset.

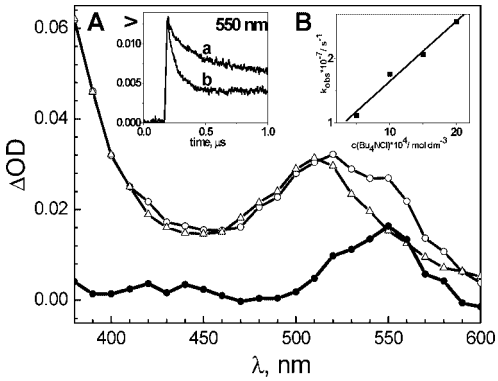

Figure 2. Transient optical absorption spectra obtained in the pulse radiolysis of N_2-saturated solution of 2-$NpNH_2$ (5×10^{-3} mol dm^{-3}) in BuCl in the absence (○) and in the presence of 1.4×10^{-3} mol dm^{-3} $Bu_4N^+Cl^-$ (Δ) taken 50 ns after the pulse. The spectrum of the radical cation (●) is given as a difference between (○) and (Δ). The insets show: (A) the decay of the 2-$NpNH_2$ radical cation in the absence (a) and in the presence (b) of $Bu_4N^+Cl^-$; and (B) Stern−Volmer-type plot for the reaction of $Bu_4N^+Cl^-$ with 2-$NpNH_2^{\bullet+}$.

nm. These two transients were tentatively classified as a solute radical cation and a solute radical, respectively. It is important to stress that both species are formed immediately after the pulse as direct products of the FET. Therefore, eq 5, describing the observed process in a simplified manner, has to be substituted by a more extended reaction scheme (eq 6) that emphasizes generation of two different products in the FET reaction (the rotating arrow symbolizes the bending motion of the hetero group $-NH_2$).

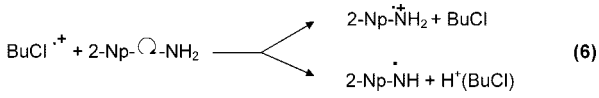

(6)

To prove our supposition about two products being formed as the result of the FET, an experiment in the presence of chloride anion as a nucleophile was performed. Thus, in the presence of 1.4×10^{-3} mol dm^{-3} $Bu_4N^+Cl^-$, a remarkable change in the spectral behavior was observed (Figure 2).

In the presence of $Bu_4N^+Cl^-$ the absorption band at 550 nm (cf. inset A in Figure 2) was considerably quenched, whereas the absorption at 510 nm was not affected. It can be explained by reaction 7:

$$Cl^- + 2\text{-}NpNH_2 \rightarrow 2\text{-}NpNH^{\bullet} + HCl \qquad (7)$$

As determined from the Stern−Volmer-type plot (inset B, Figure 2), the rate constant of reaction 7 is about 1×10^{10} dm^3 mol^{-1} s^{-1}. On the basis of the described experiment, the absorption of the short-living transient at 550 nm was attributed to the 2-$NpNH_2^{\bullet+}$ radical cation, whereas the long-lasting absorption at 510 nm was caused by the 2-$NpNH^{\bullet}$ radical. The absorption band at 370 nm (cf. Figure 2) seems to be caused predominantly by the 2-$NpNH^{\bullet}$ radical species and, therefore, does not exhibit any remarkable changes in the presence of $Bu_4N^+Cl^-$.

Analogous pulse radiolysis studies performed with 1-$NpNH_2$ in n-BuCl solution also revealed the simultaneous formation of the solute radical cations and the corresponding solute radicals. The strong superposition of the absorption of the transients in this case made kinetic analysis of the data more complex. Nevertheless, the absorption bands of the short-living transient at 370, 440, and 620 nm can be assigned to the 1-$NpNH_2^{\bullet+}$ radical cation. The long-living absorption at 400 and 540 nm belongs to the 1-$NpNH^{\bullet}$ radical. Figure 3 shows the transient spectra obtained in the pulse radiolysis of 1-$NpNH_2$ together with time profiles taken at selected wavelengths.

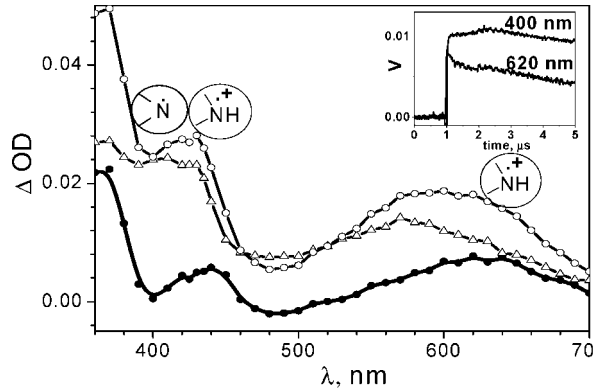

Figure 3. Transient optical absorption spectra obtained in the pulse radiolysis of N_2-saturated solution of 1-$NpNH_2$ (5×10^{-3} mol dm^{-3}) in BuCl: (○) 170 ns, (Δ) 3,4 μs after the pulse. The spectrum of the 1-$NpNH_2$ radical cation (●) is given as a difference between (○) and (Δ). Experimental time profiles are given in the inset.

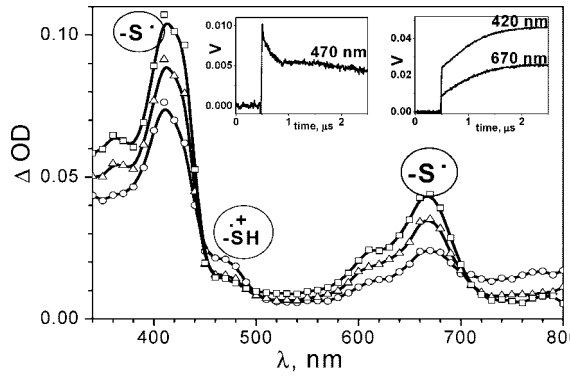

Figure 4. Transient optical absorption spectra obtained in the pulse radiolysis of N_2-saturated solution of 1-NpSH (5×10^{-3} mol dm^{-3}) in BuCl. Spectra correspond to times (○) 100, (Δ) 300, and (□) 500 ns after the pulse. Experimental time profiles taken at the absorption maxima of the observed transients are given in the inset.

1-Thionaphtol as Electron Donor. Pulse radiolysis of a 5×10^{-3} mol dm^{-3} solution of 1-thionaphtol in n-BuCl produces the transient absorption spectra shown in Figure 4.

The spectrum taken after 100 ns exhibits several pronounced absorption bands with λ_{max} at 340, 420, 470, and 670 nm, as well as a shoulder at 620 nm. These main absorption bands were assigned to the 1-thionaphtol radical cation and thionaphtyl radical formed as direct products of the FET (reaction 8).

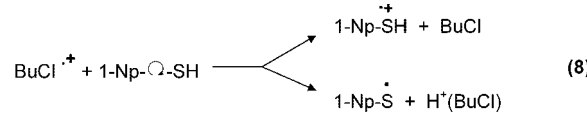

(8)

However, a marked difference in the kinetic behavior of the transients absorbing at 470 nm and at 420 and 670 nm was observed (insets in Figure 4). The time profiles give clear evidence for a delayed formation of the major part of the absorption bands at 420 and 670 nm. Such a delayed generation of the transient absorbing at 420 and 670 nm is attributed to the H-atom abstraction from 1-NpSH caused by $Bu^{\bullet}$ radicals (reaction 9), as it was already shown for several aromatic thiols.[11] Butyl radicals are the products of the solvent radiolysis (reaction 4).

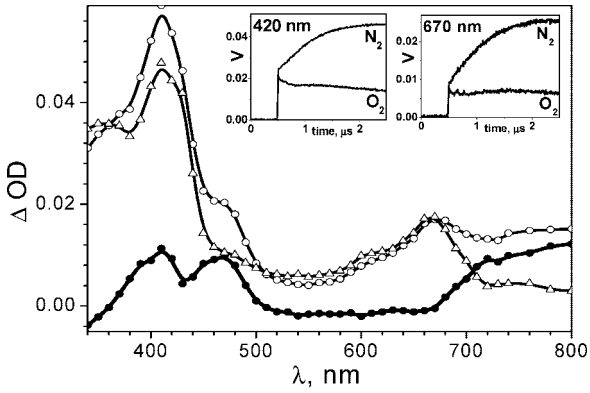

Figure 5. Transient optical absorption spectra obtained in the pulse radiolysis of O_2-saturated solution of 1-NpSH (5×10^{-3} mol dm^{-3}) in BuCl. Spectra correspond to times (○) 300 ns and (Δ) 1 μs after the pulse. The spectrum of the radical cation (●) is given as a difference between (○) and (Δ). Experimental time profiles taken at the absorption maxima of the transients are given in the insets.

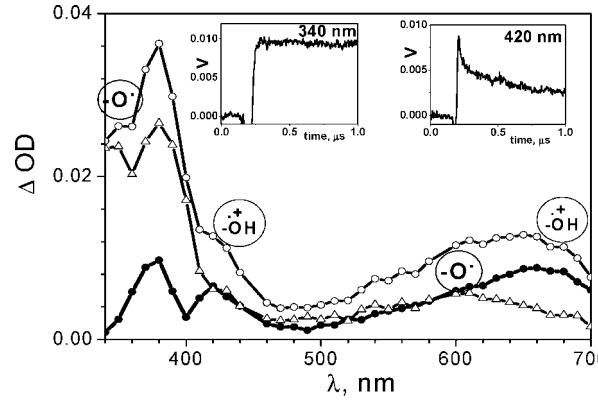

Figure 6. Transient optical absorption spectra obtained in the pulse radiolysis of N_2-saturated solution of 1-NpOH (5×10^{-3} mol dm^{-3}) in BuCl. Spectra correspond to times (○) 130 ns and (Δ) 750 ns after the pulse. The spectrum of the radical cation (●) is presented as a difference between (○) and (Δ). Experimental time profiles taken at selected wavelengths are given in the insets.

$$Bu^{\bullet} + 1\text{-NpSH} \rightarrow BuH + 1\text{-NpS}^{\bullet} \quad (9)$$

The different kinetic behavior of the transient allowed us to attribute bands at 420 and 670 nm to the thionaphtyl radicals, whereas bands at 470 and 760 nm were assigned to the short-living 1-NpSH radical cations.

The rate constant of the bimolecular reaction 9 was determined to be in the range of $(1 - 2) \times 10^8$ dm^3 mol^{-1} s^{-1}. Similar rate constants were reported for the analogous reactions of thiophenols.[11]

To avoid superposition of the ionic and the radical pathway of 1-NpS$^{\bullet}$ formation (reactions 8 and 9, respectively), radiolysis of 5×10^{-3} mol dm^{-3} solution of 1-thionaphtol in n-BuCl in the presence of oxygen was performed (Figure 5).

In an oxygen-saturated solution, parent butyl radicals are rapidly transformed into butylperoxyl radicals (reaction 10).

$$Bu^{\bullet} + O_2 \rightarrow BuOO^{\bullet} \quad (10)$$

Alkylperoxyl radicals do not react with 1-thionaphtol on the short time scale (≤ 1 ms). Therefore, the spectra given in Figure 5 are caused by transients formed only in the ionic reaction channel (eq 8). Oxygen has a marked quenching effect on that part of the absorption bands at 420 and 670 nm, which is formed in a delayed manner. Under suppression of the radical reaction channel (eq 9), the absorption bands of the radical cation at 400, 470, and 750 nm became more visible. Nevertheless, as can be seen on the insets in Figure 5 a distinct part of 1-NpS$^{\bullet}$, formed directly after the pulse in parallel with 1-NpSH$^{\bullet+}$, is still present in the system. These experimental data confirm that the FET occurs as depicted by reaction 8. The determined rate constant of this process amounts to $k_8 = (1 - 2) \times 10^{10}$ dm^3 mol^{-1} s^{-1}.

The nature of the absorption band at 470 nm was confirmed by an experiment made in the presence of 5×10^{-3} mol dm^{-3} $Bu_4N^+Cl^-$ in 1×10^{-2} mol dm^{-3} 1-NpSH solution in n-BuCl. As expected, in the presence of the nucleophile Cl^-, the decay of 1-NpSH$^{\bullet+}$ ($\lambda_{max} = 470$ nm) was accelerated due to reaction 11, whereas the absorption bands of 1-NpS$^{\bullet}$ were not affected.

$$Cl^- + 1\text{-NpSH}^{\bullet+} \rightarrow 1\text{-NpS}^{\bullet} + HCl \quad (11)$$

Ionization of 1-Naphtol. Irradiating an n-butylchloride solution of 1-naphtol (1-NpOH), we obtained the transient spectra given in Figure 6.

The spectrum taken 100 ns after the pulse shows several absorption bands with maxima at 380 and 420 nm and a broad absorption band at 550−700 nm region. The maximum observed at 380 nm appears to be a superposition of two bands caused by different transients. The kinetic analysis of the time profiles enables us to distinguish the spectrum of the short-living species with $\lambda_{max} = 420$ and 660 nm (assigned to the 1-NpOH$^{\bullet+}$) from the long-living species with $\lambda_{max} = 340$ and 600 nm, identified as corresponding 1-NpO$^{\bullet}$ radicals.[14] As one can notice, both transients (radical cation and radical) are formed simultaneously soon after the electron pulse, as the FET from 1-NpOH to BuCl$^{\bullet+}$ completes.

Discussion

Properties of FET. In a brief manner, some information concerning the properties of FET was already given in the Introduction. For the better understanding of this phenomenon, however, some crucial points should be highlighted here.

First of all, the overall reaction of FET has to be analyzed in terms of single elementary steps, as it is shown by eq. 3:

(a) The diffusional approach of the reactants is the slowest, rate determining step of FET proceeding within a few tens of nanoseconds. Quantitatively, the influence of this elementary step is reflected in the observed rate constant values of $k_2 = (1-2) \times 10^{10}$ dm^3 mol^{-1} s^{-1} for the studied compounds.

(b) As far as the radical cations derived from alkanes and alkyl chlorides are concerned, equal spin distribution over the whole molecule in these σ bond systems as well as large ionization potential differences between the donor and the acceptor (normally more than 0.5 eV) impose an unhindered electron transfer step. Such an electron jump happens in the sub-femtosecond time range in the first encounter between the reaction partners. The electron jump seems to be irreversible. The kinetics of the FET phenomenon exhibits some similarities with the one in gas phase,[15] such as collision kinetics and negligible solvation shell. However, the liquid nonpolar medium is involved in rapid thermalization and relaxation of the species. FET is a case of nonadiabatic electron transfer, which happens even on the long distance and does not form the defined encounter state[16] in the usual understanding.

(c) On the product side, the FET results in the formation of solute radical cations of different stability. The comparison between the rotational (bending) motions in donor molecules and the actual electron jump in FET shows that the latter one

is much faster. Thus, primarily the vertical ionization creates a variety of conformer radical cations with the geometry of their precursors. A simplification of this complex situation allows us to distinguish two extreme conformers: the metastable planar one and the twisted dissociative radical cation, with the spin preferably localized on the heteroatom.

(d) The metastable type of the radical cation undergoes relaxation and decays within the nanosecond time range via different channels, for example, via neutralization assisted by the negatively charged counterion. The dissociative one, however, deprotonates within the first vibrational motion of the critical bond, that is, in some femtoseconds.

Kinetic Simulation of the Data. Product Distribution after FET. As already mentioned in the introduction, a parallel generation of phenol radical cations and corresponding phenoxyl radicals has been observed in various experiments with phenol-type (ArOH) compounds.[1] Independent of the type of the nonpolar solvent[17] and the substituents at the aromatic ring,[18] the ratio between phenol radical cations and phenoxyl radicals, formed promptly, is 1:1. The given ratio between the FET products was calculated on the basis of kinetic simulations.

To achieve better understanding of the experimental data and to estimate the product ratio after FET, ACUCHEM[19] simulations of the transient kinetics at different wavelengths were performed for 2-naphtol, 2-naphtylamine, and 2-thionaphtol (see Figure 7a−c, respectively). ACUCHEM is a program solving a set of differential equations. Each equation represents an elementary reaction introduced into the reaction scheme. Rate constants for the electron transfer from the studied compounds to n-$BuCl^{\bullet+}$ radical cations as well as rate constants for other relevant processes were determined by analyzing experimental kinetic traces taken at various solute concentrations at different wavelengths and in selected cases by using Stern−Volmer-type plot. Thus, a set of known rate constants was brought together and introduced into the ACUCHEM input file as a probable reaction scheme (cf. reactions given below). Further on simulations were performed in order to obtain the best correlation between the simulated curve and the experimental time profile.

1. Ionization. Reactions of Primary Species.

$$BuCl^{\bullet+} \rightarrow \text{self decay} \rightarrow Bu^{\bullet+},\ HCl \qquad k_{12} = 8\times10^{6} s^{-1} \quad (12)$$

$$e_{solv} + BuCl \rightarrow Cl^{-} + Bu^{\bullet} \qquad k_{13} = 5\times10^{9}\ dm^{3}\ mol^{-1}\ s^{-1} \quad (13)$$

2. Interaction of Primary Species with Solute Molecules.

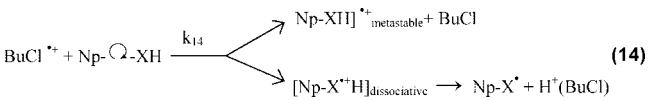

(14)

$$k_{14} = 2\times10^{10}\ dm^{3}\ mol^{-1}\ s^{-1}$$

$$Bu^{\bullet} + \text{2-NpSH} \rightarrow BuH + \text{2-NpS}^{\bullet} \qquad k_{15} = 1\times10^{8}\ dm^{3}\ mol^{-1}\ s^{-1} \quad (15)$$

$$NpXH]^{\bullet+} + Cl^{-} \rightarrow NpX^{\bullet} + HCl \qquad k_{16} = 1\times10^{10}\ dm^{3}\ mol^{-1}\ s^{-1} \quad (16)$$

*for 2-NpOH, $k_{16} = 5\times10^{9}\ dm^{3}\ mol^{-1}\ s^{-1}$

$$2NpX^{\bullet} \rightarrow \text{recombination products} \qquad k_{17} = 2\times10^{9}\ dm^{3}\ mol^{-1}\ s^{-1} \quad (17)$$

NpXH = 2-NpOH, 2-NpSH, or 2-$NpNH_2$

The rate constant for reaction 17 refers only to 2-$NpNH_2$ and 2-NpSH. Recombination does not play a significant role in the consumption of the naphtoxyl radicals.

Kinetics of the formation and the decay of the radical cations and the corresponding radicals can be expressed by the following differential equations:

$$d[NpXH^{\bullet+}]/dt = k_{14}[NpXH][BuCl^{\bullet+}] - k_{16}[NpXH^{\bullet+}][Cl^{-}]$$

$$d[NpX^{\bullet}]/dt = k_{14}[NpXH][BuCl^{\bullet+}] + k_{16}[NpXH^{\bullet+}][Cl^{-}] - k_{17}[NpX^{\bullet}]^{2}$$

For 2-NpSH:

$$d[NpS^{\bullet}]/dt = k_{14}[NpSH][BuCl^{\bullet+}] + k_{15}[NpSH][Bu^{\bullet}] + k_{16}[NpSH^{\bullet+}][Cl^{-}] - k_{17}\times[NpS^{\bullet}]^{2}$$

The experimental time profiles chosen for simulation consist of the kinetic traces of the short-living ($NpXH^{\bullet+}$) and the long-living ($NpX^{\bullet}$) transients since at the relevant wavelengths the absorption of both transients strongly overlaps (Figure 7a−c). Whereas the experimental time profiles represent only the superposition of the kinetic behavior of both absorbing intermediates, the simulation procedure allows us to separate the experimental time profiles of the kinetic traces of each of the absorbing transients. Introducing reasonable molar absorption coefficients of the short- and long-living intermediates at the analyzed wavelengths, the ratio between the two channels of the FET reaction 14 could be determined. On the given time profiles, the synchronous formation of the solute radical cations and the corresponding radicals (reaction 14) as the direct products of the FET is clearly demonstrated. The metastable solute radical cations decay due to the reaction with chloride anions (eq 16). In the course of this neutralization reaction, corresponding solute radicals are formed in a delayed manner, which is clearly seen in Figures 7a−c. The formation of the 2-$NpS^{\bullet}$ radicals via H-abstraction (reaction 15) was also taken into account.

Hence, the ratio between two channels of the FET reaction 14 could be derived from the rapid and the delayed part of the radical absorption. The following data were obtained:

2-napthol 2-$NpO^{\bullet}$: 2-$NpOH^{\bullet+}$ = 55 : 45

2-napthylamine 2-$NpNH^{\bullet}$: 2-$NpNH_2{}^{\bullet+}$ = 58 : 42

2-thionaphtol 2-$NpS^{\bullet}$: 2-$NpSH^{\bullet+}$ = 55 : 45

Interpretation of FET by Means of Quantum Chemical Calculations. With a set of the experimental results presented above, it was tempting to perform a comparison of the FET involving naphthalene derivatives (NpOH, $NpNH_2$, and NpSH; only β isomers were chosen for this purpose) with their benzene analogues (PhOH, $PhNH_2$, and PhSH). This comparison was supplemented with quantum chemical calculations on the intramolecular dynamics. Quantum chemical calculations for the ground-state molecules and their radical cations were performed by means of B3LYP/6−31G(d) method.[20] Table 1 contains a collection of data regarding calculated intramolecular

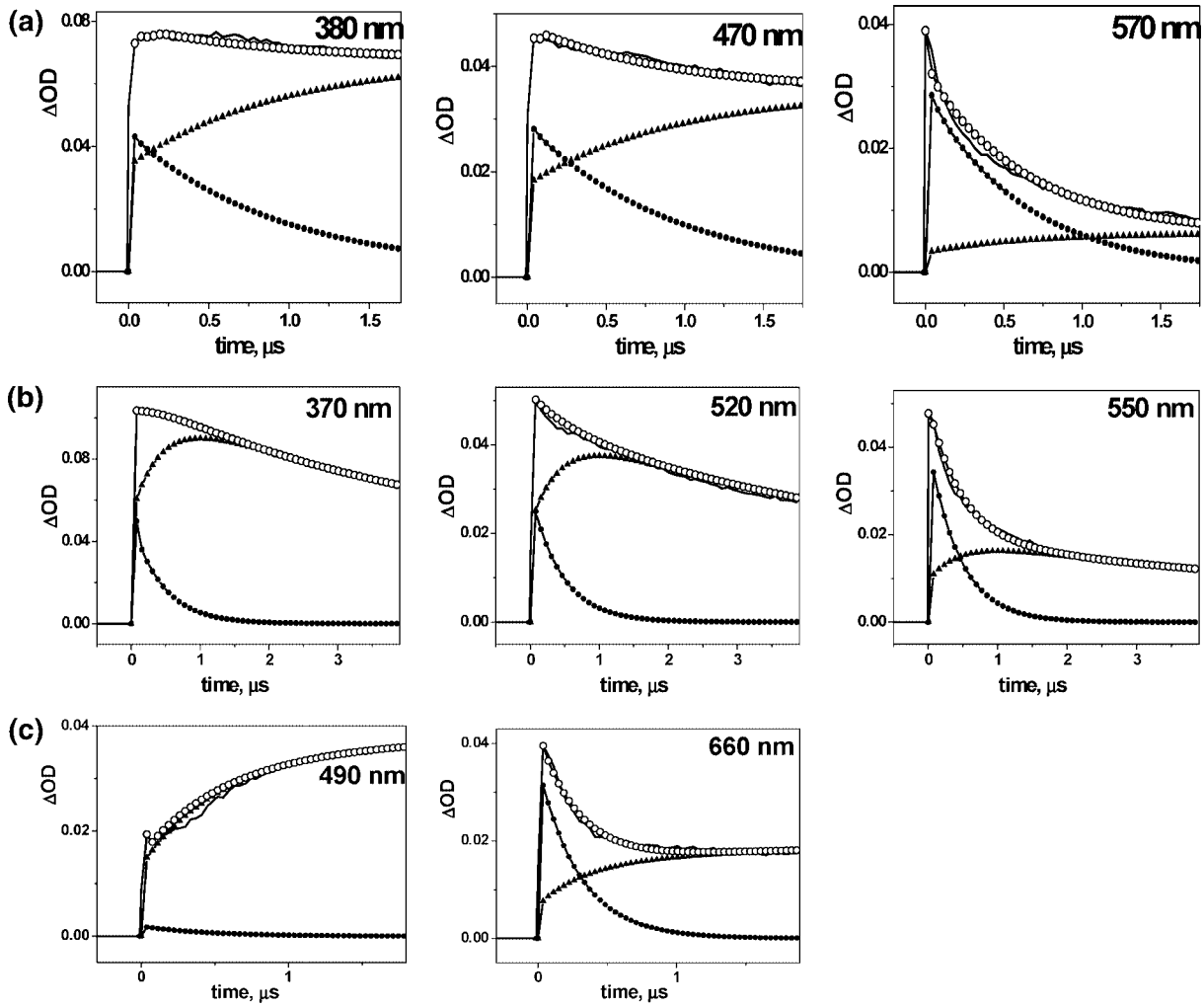

Figure 7. (a) Simulation of the experimental time profiles obtained in pulse radiolysis of N_2-saturated solution of 2-NpOH (5×10^{-2} mol dm^{-3}) in BuCl: (−) experimental profile, (○) simulated curve, (▲) 2-naphtoxyl radical, (●) 2-naphtol radical cation. (b) Simulation of the experimental time profiles obtained in pulse radiolysis of N_2-saturated solution of 2-NpNH_2 (5×10^{-3} mol dm^{-3}) in BuCl: (−) experimental profile, (○) simulated curve, (▲ 2-naphtylaminyl radical, (●) 2-naphtylamine radical cation. (c) Simulation of the experimental time profiles obtained in pulse radiolysis of N_2-saturated solution of 2-NpSH (2×10^{-3} mol dm^{-3}) in BuCl: (−) experimental profile, (○) simulated curve, (▲) 2-thionaphtyl radical, (●) 2-thionaphtol radical cation.

TABLE 1: DFT B3LYP/6-31G(d) Calculated Quantum Chemical Data

					E_a, kJ mol^{-1}				
solute	ν_{Rot}, cm^{-1}	t_{Rot}, 10^{-15} s	ν_{Vib}, cm^{-1}	t_{Vib}, 10^{-15} s	ground state	radical cation	product ratio (+•):(•)[a]	lifetime of ArXH$^{+\bullet}$[a]	S(X)[b]
$PhNH_2$	270	123	3458	9.6	23.9	152.8	50:50	400 ns	0.353
2-NpNH_2	279	119	3499	9.5	24.3	97.1	42:58	1.5 μs	0.204
PhOH	345	97	3601	9.3	13.4	62.0	50:50	280 ns	0.197
2-NpOH	369	96	3746	8.9	3.3	38.4	45:55	2.0 μs	0.102
PhSH	113	294	2591	12.8	1.7	92.1	35:65	150 ns	
2-NpSH	138	241	2695	12.3	4.2	42.3	45:55	1.0 μs	0.237

[a] Experimental values. [b] Spin density at the heteroatom.

dynamic parameters (frequencies (ν) and corresponding times (t) for the rotational (rot) and vibrational (vib) motions), values of the activation energy (E_a) for the rotation around the "aromatic moiety − heteroatom" bond (Ar−X) and the atomic spin densities S(X) on the heteroatoms. Additionally, experimentally obtained values of the lifetimes of the metastable radical cations $Ar^{\bullet+}$ and product ratios (between promptly formed radical cations and corresponding radicals) are also given.

The molecular structures appear as a complex mixture of rotational conformers. However, for the purpose of simplification, the real situation is reduced to two extreme geometries of the molecules: a planar and a twisted one. This approach was already mentioned in the Introduction. It is well justified because it reflects the real product situation.

A potential energy diagram describing energetic aspects of the FET is presented in Figure 8.

As can be seen from the data presented in Table 1, for all the studied compounds, the barrier for the internal rotation (E_a) in the ground nonionized state is relatively low. For example, in case of 2-naphtol this parameter equals 3.3 kJ mol^{-1} (cf. Table 1). Such values of the activation energy for the rotation are low

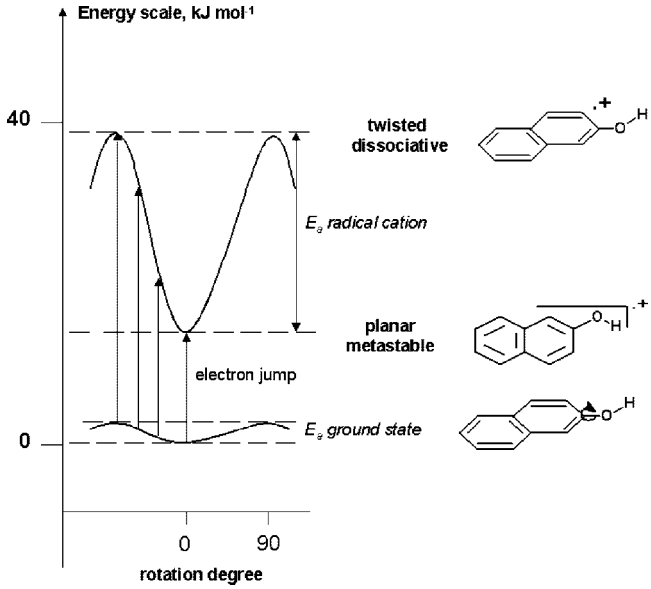

Figure 8. Potential energy diagram depicting the energetics of the donor (2-naphtol) in the ground and in the radical cation state. The influence of the rotational angle on the energetic state of the radical cation is demonstrated.

enough, so that at room temperature the compounds exist in solution as a diversity of rotational conformers. In contrast, after ionization the rotational motion is strongly hindered by the increased activation barrier (up to 38.4 kJ mol^{-1} for 2-naphtol). It does not mean that the geometry of the radical cation becomes fixed, just that the reorganization of the planar type of the radical cation into the twisted one appears to be improbable because of energetic reasons. The planar radical cation is metastable and can be found in the minimum of the potential energy surface. Contrarily, the twisted radical cation lies at a higher energetic level. The frequency of the rotational motion of the substituent toward the aromatic ring is not changed significantly after the ionization. Hence, the radical cation in its unstable twisted conformation has an opportunity to transform into the metastable planar form. However, this reorganization process has to compete with very fast dissociation of the twisted unstable radical cation, since the valence vibrations of the X−H (heteroatom−hydrogen) bond are at least 10 times faster than the rotation around the Ar−XH bond (cf. Table 1). In principle, deprotonation of the twisted unstable radical cation should occur within the first vibrational motion. In this process n-BuCl acts as proton acceptor. Because of the influence of the solvent and the very fast vibrational motions compared to the rotational ones, the energetically unfavorable (endothermic) self-deprotonation takes place, that is, the kinetic factor dominates over the thermodynamic one. These considerations are valid for the naphthalene derivatives as well as their benzene analogues.

As can be seen from Table 1, the rotational and the vibrational frequencies are very similar for benzene and naphthalene derivatives possessing the same heteroatom. Apparently, the change in the size of the aromatic moiety does not remarkably affect the intramolecular dynamic parameters.

Comparing the ratio between the radical cation and the corresponding radical formed in the FET reaction for benzene and naphthalene compounds, a distinct difference can be noticed. The ionization of phenol and aniline generates radical ions and radicals in equal amounts. In the case of thiophenol, the radical fraction prevails over the ionic one. Because of the presence of sulfur, being a heavier atom, an unpaired electron is more pronouncedly localized on the heteroatom, which facilitates

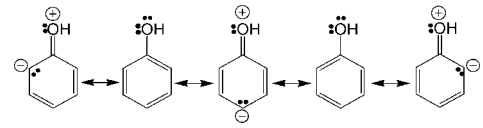

Figure 9. Structures contributing to the resonance hybrid of phenol.

deprotonation. The product ratio obtained for naphthalene compounds shows that the radical fraction slightly dominates over the radical cationic one. However, this effect should not be overestimated because it lies more-or-less within the error value of the fitting procedure.

A difference between benzene and naphthalene compounds can be observed as far as the lifetimes of the metastable radical cations are concerned. In the case of benzene compounds, the radical ions decay within some hundreds of nanoseconds, whereas the naphthalene-derived radical cations exist in the range of some microseconds. The lifetimes of the metastable radical cations are clearly connected with the spin density at the heteroatom S(X). In detail, an inverted correlation between the lifetime value of the solute radical cation and the spin density at the heteroatom is observed, that is, an increase of the spin density at the heteroatom shortens the lifetime of the radical cation.

Resonance and FET. Here, one of the consequences of the FET phenomenon should be discussed. This will be done by comparing the usual treatment of electronic effects (resonance) with the peculiatities of the FET.

Commonly, the electron distribution in substituted aromatics such as phenols, thiophenols, aromatic amines, etc. is described in terms of the concept of resonance[21] (alternatively called mesomerism or delocalization). In other words, such aromatic systems are assumed to exist as mesomeric states in which π- and n-electrons are involved in resonance. This concept provides a simple way of representing the structures graphically, cf. Figure 9. Here, all borderline structures of the phenol molecule symbolize the assumed resonance. These structures are considered to be planar. Certainly, today the electron distribution can be calculated by quantum chemical methods, resulting in a more precise picture.[22]

The thermodynamically justified property enables the reasonable interpretation of bimolecular reactions occurring in the time range upward of nanoseconds, which is typical for most of the diffusion-controlled bimolecular processes.[15]

In the FET, however, the electron jump and, therefore, the chemical reaction proceeds in the subfemtosecond time range. As already mentioned, this identifies the molecules in the dynamic situation of intramolecular oscillations, which take place in the femtosecond time domain, that is, they are significantly slower than the electron jump. Hence, the studied compounds constitute a dynamic mixture of conformers with different rotational angles between the substituent and the aromatic ring. The fate of the product radical cations of the donor molecules is determined by this actual angle of twist and, therefore, metastable and dissociative radical cations can be distinguished. The latter ones decay immediately in the early femtosecond time range due to the vibrational motion of the critical bond. Therefore, the product distribution is kinetically controlled, that is, it is determined by the time domains of the events, and the rules of mesomerism on such a short time scale cannot be applied.

In contrast to nonpolar media, in polar systems the encounter complex plays a deciding role governing the mechanism of the electron transfer. The ions are stabilized by the solvation shell.

The electron transfer proceeds after a set of interactions of the reaction partners. An encounter complex between the reactants is formed with an energetically optimized and more rigid structure. The electron jump proceeds in a delayed manner compared to the FET, where such a defined complex is not formed.

In light of these considerations, it can be stated that mesomerism is a property of the encounter complex. At least in nonpolar systems the isolated molecules should be described in terms of dynamic motions rather than of mesomeric states. So the FET in nonpolar media seems to offer a new aspect in the interpretation of the term "mesomerism" in chemical reactions, which should be analyzed in more detail in future.

Conclusions

Free electron transfer involving aromatic compounds with an extended aromatic moiety—substituted naphthalene derivatives (naphtylamines, naphtols, and thionaphtols)—was studied with electron pulse radiolysis. It was found that naphtyl-substituted radical cations exhibit higher stability (longer life times) in comparison to the analogous phenyl derivatives.

In analogy to the former investigations, two direct products of the FET were observed, that is, solute radical cations and the corresponding heteroatom-centered radicals. This two-product situation is explained by an unhindered electron jump taking place in the first encounter of the reactants, which reflects the molecular dynamic behavior of the donor molecules in the ground-state leading to the generation of the solute radical cations with different stabilities. Since in the ground-state the molecules represent a dynamic mixture of the rotational conformers, the rapid ionization of these different conformer states results in the simultaneous formation of two types of donor radical cations, that is, metastable and dissociative ones.

DFT calculations on the intramolecular dynamics of the studied naphthalene compounds enable the detailed understanding of the mechanism of the FET in nonpolar systems. Overall, it appears a somewhat paradox situation where the femtosecond molecular dynamics is reflected in a bimolecular electron transfer process proceeding in the nanosecond time range.

References and Notes

(1) Brede, O.; Naumov, S. *J. Phys. Chem. A.* **2006**, *110*, 11906.
(2) Mehnert, R. In *Radical Ionic Systems—Properties in Condensed Phases*; Lund, A., Shiotani, M., Eds.; Kluwer Academic Publishers: Dordrecht, The Netherlands, 1991; p 231.
(3) Trifunac, A. D.; Sauer, M. C.; Shrob, I. A.; Werst, D. W. *Acta Chem. Scand.* **1997**, *51*, 158.
(4) Arai, S.; Kira, A.; Imamura, M. *J. Phys. Chem.* **1976**, *80*, 1968.
(5) *Handbook of Chemistry and Physics*, *73*rd ed.; Lide, D. R. Ed.; CRC Press: Boca Raton, 1992; pp 10—214.
(6) Warman, J. M.; Infelta, P. P.; de Haas, M. P.; Hummel, A. *Can. J. Chem.* **1997**, *55*, 2249.
(7) Zador, E.; Warman, J. M.; Hummel, A. *Chem. Phys. Lett.* **1973**, *23*, 363.
(8) Turro, N. J. *Modern Molecular Photochemistry*; University Science Books: Mill Valley, CA, 1991; p 6.
(9) Karakostas, N.; Naumov, S.; Siskos, M. G.; Zarkadis, A. K.; Hermann, R.; Brede, O. *J. Phys. Chem. A.* **2005**, *109*, 11679.
(10) Karakostas, N.; Naumov, S.; Brede, O. *J. Phys. Chem. A.* **2007**, *111*, 71.
(11) Hermann, R.; Dey, G. R.; Naumov, S.; Brede, O. *Phys. Chem. Chem. Phys.* **2000**, *2*, 1213.
(12) Mohan, H.; Hermann, R.; Naumov, S.; Mittal, J. P.; Brede, O. *J. Phys. Chem. A.* **1998**, *102*, 5754.
(13) Farhataziz M. A.; Rodgers, J. *Radiation Chemistry, Principles and Applications*; VCH Publishers: Weinheim, 1987.
(14) Das, T. N.; Neta, P. *J. Phys. Chem. A.* **1998**, *102*, 7081.
(15) Levine, R. D.; Bernstein, R. B. *Molekulare Reaktionsdynamik*; Teubner: Stuttgart, 1991; p 44.
(16) Kavarnos, G. J. *Fundamentals of Photoinduced Electron Transfer*; VCH Publishers: New York, 1993; p 53.
(17) Ganapathi, M. R.; Hermann, R.; Naumov, S.; Brede, O. *Phys. Chem. Chem. Phys.* **2000**, *2*, 4947.
(18) Brede, O.; Ganapathi, M. R.; Naumov, S.; Naumann, W.; Hermann, R. *J. Phys. Chem. A.* **2002**, *106*, 1398.
(19) Braun, W.; Herron, J. T.; Kahaner, D. K. *Int. J. Chem. Kin.* **1988**, *20*, 51.
(20) Becke, A. D. *J. Chem. Phys.* **1996**, *104*, 1040.
(21) Kerber, R. C. *J. Chem. Educ.* **2006**, *83*, 223.
(22) Brede, O.; Hermann, R.; Naumann, W.; Naumov, S. *J. Phys. Chem. A* **2002**, *106*, 1040.

JP806711M